Electronic Supplementary Material (ESI) for Chemical Communications.

Electronic Supplementary Information

Cross-β Amyloid Nanotubes for Hydrolase -Peroxidase Cascade

Ayan Chatterjee, Syed Pavel Afrose, Sahnawaz Ahmed, Akhil Venugopal and Dibyendu Das*

Department of Chemical Sciences and Centre for Advanced Functional Materials, Indian Institute of Science Education and Research (IISER) Kolkata, Mohanpur 741246, India

Email: dasd@iiserkol.ac.in

Table of Contents

1.	Materials	3
2.	Methods	3
2.1.	Synthesis	4
2.2.	Peptide assembly	4
2.3.	Redispersion technique	5
2.4.	Gold nanoparticle binding	5
2.5.	Experimental methods	6
2.6.	HFIP study	13
2.7.	Peptide bundling	13
2.8.	Inhibition study	13
2.9.	Time delayed addition	14
2.10.	Delayed association of hemin	14
3.	Table	15
4.	CD and FTIR	16
5.	HPLC chromatograms and mass spectra of purified peptides	18
6.	TEM images	18
7.	Confocal images	19
8.	Hemin loading and bar diagram	20
9.	UV-Visible spectra	21
10.	HPLC chromatogram of oxidized product	21
11.	Lineweaver-Burk plots	22
12.	pH rate profile	24
13.	UV-Vis of hemin in HFIP treated peptide	27
14.	Bar diagram of the hydrolysis rates	29

General descriptions

1. Materials

All fluorenylmethyloxycarbonyl (Fmoc) protected amino acids, activator HCTU [2-(6-chloro-1H-benzotriazol-1-yl)-1, 1, 3, 3-tetramethylaminium-hexafluorophosphate], DIPEA (*N*, *N*-diisopropylethylamine), piperazine, trifluoroacetic acid (TFA), 1,1,1,3,3,3-Hexafluoro-2-propanol (HFIP), gold chloride trihydrate, sodium borohydride and trisodium citrate dihydrate, fluorophore coumarin 343, hemoglobin human were purchased from Sigma Aldrich. Cytochrome C (Oxidized) ex. Horse Heart extrapure, Hemin cryst. Ex. Bovine, Peroxidase ex. Horseradish and other chemicals were purchased from SRL India. Hydrogen peroxide (30%, w/v solution), all solvents and Fmoc-Rink amide MBHA Resin were purchased from Merck. Milli-Q water was used throughout the experiments. Positively charged gold nanoparticles of 10 nm size functionalized with (11-Mercaptoundecyl)-*N,N,N*-trimethylammonium bromide were procured from Cytodiagnostics, Canada.

2. Methods

2.1. Synthesis

2.1.1. Synthetic procedure of peptides

The peptides were synthesized manually by conventional Fmoc solid phase synthesis at elevated temperature (65 °C) using Fmoc-Rink Amide Resin. Resins were suspended and allowed to swell in dimethylformamide (DMF) for 30 min followed by Fmoc deprotection with 20% piperazine-DMF mixture. Amino acid coupling on the resin surface was carried out by using HCTU and DIPEA maintaining 65 °C. Each coupling step involved thorough washing of resins with DMF prior to addition of amino acid. After the final amino acid coupling is done, the terminal Fmoc group was removed using 20% piperazine-DMF followed by washing with DMF. Acetylation of the N -terminus was done by using 20% acetic anhydride in DMF. Cleaving of the peptides from resins was done in dichloromethane in presence of TFA/thioanisole/1,2-ethanedithiol/anisole (90: 5 : 3 : 2, v/v/v/v) at room temperature

for 3 h. The resins were removed by filtration and peptide was precipitated out from the solution by adding ice cold diethyl ether. The precipitated product was centrifuged at 7000 rpm for 10 min, and the pellet was further washed 3 times with cold diethyl ether. The crude peptides were purified on a preparative Waters HPLC system with Atlantis T3 C18 preparative reverse phase column, using a linear gradient of water containing 0.1% TFA and acetonitrile containing 0.1% TFA.

Ac-**H**LVFFA**L**-NH_2 (**HL**) (m/z) calculated for [M+H^+]: 887.51; found: 887.51

Ac-**K**LVFFA**L**-NH_2 (**KL**) (m/z) calculated for [M+H^+]: 878.54; found: 878.55

Ac-**H**LVFFA**E**-NH_2 (**HE**) (m/z) calculated for [M+Na^+]: 925.47; found: 925.43

Ac-**HH**LVFFA**E**-NH_2 (**HHL**) (m/z) calculated for [M+H^+]: 1024.57; found: 1024.56 for [M+H^+] and 512.79 for [M+2H^+].

2.1.2. Synthesis of 2-methoxy phenyl acetate (MPA)

Glacial acetic acid (254 µL), *N*, *N*'-dicyclohexylcarbodiimide (1244 mg) and 4-dimethylaminopyridine (488 mg) were dissolved in ethyl acetate (20 mL)-DMF (1 mL) mixture and stirred at 0 °C for 20 min. 2-Methoxy phenol (450 µL) was then added and allowed to stir for 16 h at room temperature. After filtration of the reaction mixture, the filtrate was concentrated, added to water and extracted with ethyl acetate. The organic layer was washed twice with brine and dried over anhydrous $MgSO_4$. The crude mixture after solvent evaporation was purified by silica gel chromatography to give a clear oil of 2-methoxy phenyl acetate (MPA).

^{1}H NMR (400 MHz, $CDCl_3$) δ (ppm) 7.04 (m, 1H), 6.95 (dd, 1H), 6.87 (m, 1H), 6.84 (dd, 1H), 3.72 (s, 3H), 2.21 (s, 3H). ESI-MS MPA (m/z) calculated for [M+Na^+]: 189.07; found: 189.21 [M+Na^+]

2.1.2. Synthesis of negatively charged gold nanoparticle

From previously published procedure negatively-charged gold nanoparticles (Neg-AuNP) were synthesized.[1,2] Diameter of the gold nanoparticles was 5 ± 2 nm. Briefly,

freshly prepared 15 µL of sodium citrate solution (100 mM) was added to a round bottom flask containing 3.82 mL of deionized water. To that, 18 µL of $HAuCl_4$ (83.8 mM) solution was added in stirring condition. To this mixture, freshly prepared ice cold solution of 150 µL $NaBH_4$ (100 mM) was added gradually under vigorous stirring condition. The solution gradually turned pink, indicating the formation of gold nanoparticles with a localized surface plasmon resonance (SPR) transition at 509 nm. Final concentration for citrate and $HAuCl_4$ was maintained at 0.3 mM and for $NaBH_4$ the final concentration was 3 mM.

2.2. Peptide assembly

In order to ensure the formation of homogenous assemblies, lyophilized powder of purified peptides were treated with HFIP which eliminated any preformed aggregates that formed during purifications. After drying, the peptide films were dissolved in 40% (v/v) acetonitrile/water having 0.1% TFA (v/v) and cyclomixed. The homogenous solutions were assembled for a month before using.

In assembled state, each peptide strand is arranged in an antiparallel conformation which exposes the charged residues at the 16^{th} position along with the 22^{nd} position of the neighboring strand towards the solvent.[1, 2]

2.3. Redispersion technique

1 mL of assembled peptide sample (2.5 mM) was taken in 1.5 mL microcentrifuge tube and was centrifuged for 15 min at 10,000 rpm (rotor F45-30-11) at 10 ºC temperature in eppendorf centrifuge 5804 R. The Pellet obtained after discarding the supernatant was redispersed in glycine HCl buffer (5 mM, pH 3).

2.4. Gold Nanoparticle binding studies

For gold nanoparticle binding studies, 200 µL of gold colloid (both positively charged and negatively charged AuNP, 0.3 mM) were separately added to 5 µL of the aqueous dispersions of nanotubes of **HL** and **KL**. The pH of the system after addition of AuNP

was found to be 8. The mixture was kept for incubation for ca. 4 h at room temperature until a purple red precipitate was formed. The mixture was centrifuged and the pellet was redispersed in water. 10 µL of this solution was carefully drop casted on TEM grids and aged for 2 min before wicking off the excess solvent with filter paper. We did not observe any signs of bundling or aggregation from the TEM micrographs despite the pH being 8. This could be due to the instantaneous binding of the Neg-AuNP with the histidine exposed surface of the nanotubes. Further deprotonated imidazoles and amines have been shown to interact with Au-NPs.[3] To probe this in detail, **HL** nanotubes were pre-incubated at higher pH (HEPES 10 mM, pH 8) for 60 min and afterwards Neg-AuNP was added. Bundles of Neg-AuNP bound nanotubes was obseved (Figure S5A).

2.5. Experimental methods

2.5.1. Transmission Electron Microscopy (TEM)

The TEM samples were prepared by drop casting the peptide assemblies on TEM grid. The solutions were aged for 1 min on the grid. Filter paper was used to wick off the excess solution followed by addition of 2 % (w/v) uranyl nitrate and incubation for 3-5 minutes. Samples were then placed in desiccators under vacuum. TEM micrographs were recorded with a JEOL JEM 2100 with a Tungsten filament at an accelerating voltage of 200 kV.

2.5.2. Scanning Electron Microscope (SEM)

The peptide samples were made by drop casting on a silicon wafer and dried overnight at room temperature. The samples were recorded on a Gemini SEM 300 (Sigma Zeiss) instrument.

2.5.3. Circular Dichroism

CD spectra were recorded using a JASCO J-810 circular dichroism spectrometer fitted with a Peltier temperature controller to maintain the temperature of 25 °C. 600

μL of the peptide samples (2.5 mM) were placed into a quartz cuvette with 1 mm path length. Each spectrum was obtained by scanning wavelength from 550 nm to 190 nm at a scanning rate of 100 nm/min. Three successive wavelength scans were taken to average for each sample. CD spectra were also recorded of hemin bound peptides samples. For CD studies of hemin, final hemin concentration was 1mM in a quartz cuvette of 10 mm path length. In Figure S1, negative band appears at 220 nm and a positive band at 190 nm, leading to a negative Cotton effect of β sheet. The intensities and energies of the n to π* (close to 220 nm) and π to π* transitions (close to 190 nm) depend on the peptide bond angles (ϕ and Ψ).[4]

2.5.4. Fourier-Transform Infrared Spectroscopy

Sample aliquots were dried as thin films to record IR spectra using Bruker (model no: Alpha) in ATR mode (Platinum ATR). Average of 256 scans with 4 cm^{-1} resolution were recorded at room temperature. Background spectra were subtracted from each sample spectrum. In Figure S2, strong absorption band of amide I at ~1625-1630 cm^{-1} is the characteristic peak of H-bonded β-sheet structures and the weak absorption at ~1685-1690 cm^{-1} is consistent with an antiparallel configuration.[5]

2.5.5. Confocal Microscopy

Briefly, 1 μL coumarin 343 dye (3.5 mM) was mixed with 10 μL of **HL** (2.5 mM) and incubated for 2 h. The solution was then casted on a glass slide and was enclosed with a cover glass. Confocal image was taken at frame of 512X512, with 12 bit depth with a 100X, Plano Apochromat objective, N.A.1.4, excited by 488 nm laser line, emission bandwidth of 493-560 nm in CLSM 710 (ZEISS Axio observer 2.0).

Shifting of UV absorbance of coumarin based dyes has been attributed to binding to hydrophobic regions. In this regard, **HL** nanotubes expose hydrophobic leucines towards the solvents due to antiparallel registry offer microenvironments for binding of hydrophobic guests like coumarin and hemin.[6,7] In this case, blue shift of UV spectrum of coumarin upon binding with nanotubes was observed (Figure S7).[6]

2.5.6. UV-Vis spectroscopy study

2.5.6.1. The UV-Visible spectra of hemin in free and bound states

The UV-Vis spectra of hemin were monitored spectrophotometrically in the AGILENT CARY 8454 UV-Visible spectrophotometer from 300 to 700 nm. The spectra of free hemin and hemin in presence of peptide assemblies were recorded. Briefly, 1.1 µL of hemin (1 mM stock in DMSO) was added in 110 µL micro volume cuvette of 10 mm path length and scans were recorded. In case of hemin bound peptide assemblies, 44 µL of peptide (stock of 2.5 mM) and 1.1 µL of hemin (1mM stock in DMSO) were mixed in presence of 64.9 µL of buffer and scans were recorded. UV-Vis spectra are background subtracted with solutions containing the corresponding peptide nanostructures (in case of free hemin at pH 3, the background was done with buffer). For scattering experiment, OD values were noted at λ=700 nm by adding the peptides in cuvette of 10 mm path length.

Similar hemin spectral pattern of hemin in water and in buffer (pH 3, glycine HCl) that shows no blue shifted peak which ruled out demetallation (Figure S9).

2.5.6.2. Hemin loading on peptide nanotubes

The amyloid nanotube surface exposes hydrophobic leucine moieties to solvent along with the charged residues.[5] These hydrophobic microdomains interact with hydrophobic guests such as hemin. Further, hemin binding has previously been shown with different kind of nanoassemblies.[7] Briefly, aqueous solutions of **HL** nanotubes (1mM, 444 µg) were exposed to various concentrations of hemin from 1 µM to 100 µM (DMSO stock) and incubated for 1 to 10 min (total volume 250 µL, amount of hemin from 0.3 to 33 µg). After incubation, ammonium hydroxide (NH_4OH, 250 µL, 1.40 N) was added to the mixture as hemin is known to be soluble in NH_4OH. We expected that the addition of NH_4OH will help in the removal of free or non-specifically bound hemin. Addition of NH_4OH resulted in increase of pH from 3 to 8. The assemblies were then shaken on a platform shaker for 1 minute and centrifuged

at 10000 rpm at 25 ^{0}C for 5 min. The supernatant was carefully removed. Typically two washes were performed, with fresh NH_4OH solution added each time to remove unbound hemin. All supernatants along with washes were analysed for hemin content using UV Vis spectroscopy with the help of a standard plot. The amount of hemin loaded onto the nanotubes was determined by calculating the difference in the hemin concentration in solution before and after exposing it to the dispersion of nanotubes in water.

2.5.6.3. Activity measurement

The activity of the hemin bound peptide assemblies was monitored with the substrates methoxy phenol (MP) and methoxy phenyl acetate (MPA) in presence of H_2O_2 in glycine HCl pH 3 buffer.[8] For the hemin histidine freely diffusing system, pH 8 was maintained by HEPES (5 mM) buffer. Briefly, 44 µL of the peptide assemblies (2.5 mM) and 60 µL of buffer solution were in a micro volume quartz cell of 10 mm path length. Then, 1.1 µL of hemin (1 mM stock in DMSO) was added. This was followed by addition of 2.75 µL MP/MPA (varying stock concentrations in acetonitrile for different final concentrations of substrate). For the free system, 44 µL of histidine (2.5 mM stock) was used instead of peptide. Finally, 1.1 µL of H_2O_2 (3 M stock, saturation concentration) was added to start the reaction. Overall concentration of the peptide in the reaction mixture was 1 mM. The absorbance change was monitored by formation of the oxidized product of methoxy phenol, at λ_{max} = 470 nm (ε at 470 nm is 26600 $M^{-1}cm^{-1}$). Varying concentration of H_2O_2 (from 10 mM to 60 mM) were similarly used for checking the activity of **HL** keeping the fixed concentration of substrate MP and MPA.

2.5.6.4. Activity measurement of hemoglobin and cytochrome C

1.1 µL protein (cytochrome c or hemoglobin, stock 1 mM) was added along with 2.75 µL of MPA / MP (varying stock concentrations for different final concentrations of substrate) to 105 µL of buffer (pH 3, glycine HCl) followed by the addition of 1.1 µL H_2O_2 (3 M stock) to initiate the reaction. Activity was measured as mentioned before. For comparison, horseradish peroxidase (HRP) was also used in a saturating MPA concentration of 25 mM along with 30 mM H_2O_2. Briefly, 1.1 µL HRP (stock 1 mM)

was added along with 2.75 µL of MPA (1 M stock in acetonitrile) to 105 µL of buffer (pH 3, glycine HCl) followed by the addition of 1.1 µL H_2O_2 (varying stock concentrations in water for different final concentrations of substrate) to initiate the reaction. The initial rate for HRP was found to be 55 ± 10 µM-min^{-1}. This rate was comparable to the hemin-**HL** system (51 ± 10 µM-min^{-1}) done in similar pH conditions at [MPA]= 25 mM, [H_2O_2]= 30 mM.

The activities of these proteins were checked at pH 7 (HEPES buffer) which showed lower activity than hemin–**HL** with MPA as a substrate (Table S1).

2.5.6.5. Kinetics Analysis:

For Oxidation of MP to tetraguaiacol

The average slope in the first minute was used to investigate V_i (initial velocity) due to the zero-order kinetics. By changing the substrate concentration from 25 mM to 5 mM, with fixed saturation H_2O_2 concentration of 30 mM, a series of initial reaction rates was measured with the assumption that the enzyme is truly saturated with H_2O_2 with no substrate inhibition from H_2O_2. The rates were then treated with the Michaelis-Menten equation (1).

$$v = \frac{k_2[E]_0[S]}{k_m + [S]} \qquad (1)$$

The turnover number, $k_{cat}=V_{max}/[E]$, was calculated by the Lineweaver-Burk plot ($1/V_i$ as y axis and 1/[S] as x axis), which is independent of substrate and enzyme concentration.

For Hydrolysis-Oxidation Cascade of MPA to tetraguaiacol:

In a simplified version, the following mechanism can be represented for the present system[4-6]

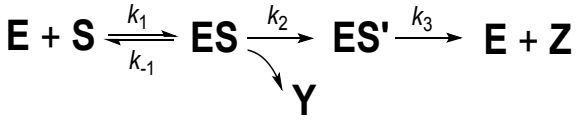

In the cascade reaction, the first product **Y** [ca. **Y** = acetic acid, **S** = 2-methoxy phenyl acetate (MPA), **S'**=2-methoxy phenol (MP)] as a result of breaking of the Michaelis complex, subsequently forms the second intermediate **ES'** (catalyst-MP complex). This second intermediate gives the colored product **Z** (tetra guaiacol) which is followed with time.

Applying the steady state approximation to this mechanism yields the rates of formation of both **Y** and **Z**, given as:

$$v = \frac{\frac{k_2 k_3}{k_2 + k_3}[E]_0[S]}{\left(\frac{k_{-1} + k_2}{k_1}\right)\left(\frac{k_3}{k_2 + k_3}\right) + [S]} \qquad (2)$$

This equation can be written in form of Michaelis-Menten form with

$$V = \frac{k_2 k_3}{k_2 + k_3}[E]_0$$

$$K_m = \left(\frac{k_2 + k_{-1}}{k_1}\right)\left(\frac{k_3}{k_2 + k_3}\right)$$

Since we found out that the second step (oxidation) is much faster than the first step (hydrolysis) ($k_3 >> k_2$) (see Figure S24-26 below), the equation 2 can be reduced to equation 1. Further, the intermediate ES' can be neglected as it exists only at very

low concentrations. Therefore, the mechanism reduces to the simple one-intermediate mechanism. [9-11]

In general, this type of rate equation can be expressed by,

$$v = \frac{k_c[E]_0[S]}{k_m + [S]}$$

Where k_c (referred in manuscript) is the catalytic constant. In fact, this equation is applicable for cascades involving any number of sequential intermediates like

$$\mathbf{E} \longrightarrow \mathbf{ES} \longrightarrow \mathbf{ES'} \longrightarrow \mathbf{ES''} \longrightarrow \text{and so on.}$$

This strategy to find the turn over number is generally used in multistep cascade reactions in biological systems.[9-14]

2.5.4.6. HPLC study:

Preparative and analytical high performance liquid chromatography (HPLC) was performed on Waters HPLC system (2535 quaternary and 1525 binary pump for preparative and analytical LC respectively) equipped with 2998 photodiode array detector and 2489 UV-Vis detector. Atlantis® T3 C18 5 μm, 4.6 X 250 mm analytical column and Atlantis® T3 Prep OBD 5 mm, 19x250 mm preparative column were used. For analytical HPLC, the flow rate was maintained at 1 mL/min with a gradient from 30 to 100 % acetonitrile in water (both solvents had 0.1 % TFA) in elution time of 20 min. Briefly, 25 mM of methoxy phenyl acetate (MPA) was added to 1 mM of the peptide (**HL**) in pH 3 buffer, and injected to HPLC at different time intervals. Increase of peak areas were measured and from a standard plot with known concentrations of MP, rates were measured. Peak area of controls without peptide at pH 3 were subtracted.

2.6. HFIP study

1 mL solution of **HL** was centrifuged for 15 min at 10,000 rpm at 10 ºC in Eppendorf centrifuge to form pellet. After discarding the supernatant, 1 mL of HFIP was added and the mixture was incubated for 1.5 h for the disassembly. HFIP was removed with a stream of N_2 gas and dried for 6 h under vacuum. Afterwards, 1 mL of buffer was added to the film of disassembled peptide to make the final concentration of **HL** to be 2.5 mM.

2.7. Peptide bundling

In microvolume cuvette, 44 µL of **HL** (2.5 mM) and 3 µL of Na_2SO_4 (25 mM) were mixed. After 10 min of incubation for bundling (bundling confirmed with TEM, Figure 3c manuscript), 58 µL of buffer was added. Afterwards, 1.1 µL of hemin (1 mM stock in DMSO) was added followed by the addition of 2.75 µL MPA (varying stock concentrations for different final concentrations of substrate). Finally 1.1 µL H_2O_2 (3 M stock in water) was added to initiate the oxidation and activity was monitored as mentioned before.

2.8. Inhibition study

Activity was monitored in 110 µL microvolume cuvette (10mm path length) where 44 µL of **HL** (2.5 mM) was mixed with 1.1 µL of hemin (1 mM stock in DMSO), 2.75 µL of MPA (varying stock concentrations for different final concentrations of substrate) and buffer (pH 3, glycine HCl). Afterwards, 2.2 µL of $NiBr_2$ (50 mM) and 1.1 µL H_2O_2 (3 M stock in water) was added simultaneously to the cuvette and activity was monitored. In case of free histidine hemin system, 44 µL of histidine (2.5 mM) was added instead of peptide. Buffer used for free system was HEPES, pH 8.

2.9. Time delayed addition of H_2O_2

For time delayed addition of H_2O_2, different vials were used. Briefly, 544 µL of buffer (pH 3) were mixed with 220 µL of **HL** (2.5 mM stock), 5.5 µL hemin (1 mM stock in DMSO) and 13.75 µL of MPA (varying stock concentrations for different final concentrations of MPA). 108.9 µL of aliquots were taken immediately after mixing, after 30 min and after 90 min and added to 110 µL of black quartz cuvette. The reactions were initiated by addition of 1.1 µL of H_2O_2 (3 M stock in water) and activity was monitored.

2.10. Delayed association of hemin

44 µL of **HL** (2.5 mM) was mixed with 61 µL of buffer (pH 3, glycine HCl) followed by the addition of 2.75 µL of MPA (varying stock concentrations for different final concentrations of substrate). The mixture was aged for 10 min. Afterwards, 1.1 µL of hemin (1 mM) was added along with 1.1 µL of H_2O_2 (3 M) and the activity was monitored. For freely diffusing system of histidine hemin, 44 µL of histidine (2.5 mM) was used instead of peptide and the buffer was HEPES, pH 8.

Table S1: The k_c value (min^{-1}) of different hemin loaded systems and proteins towards varying concentrations of methoxy phenol (MP) and methoxy phenyl acetate (MPA). [Hemin]=0.01 mM, [H_2O_2] =30 mM. Protein concentrations were kept at 0.01 mM at pH 3.

System	k_c (MP)	k_c (MPA)
Hemin-**HL**	14.5 ±0.9	7.7 ±0.7
Hemin-**KL**	0.5 ±0.03	0.08 ±0.007
Hemin-**KL**+His	11.5 ±0.8	0.21 ±0.02
Hemin-**HE**	7.22 ±0.65	0.14 ±0.01
Hemin-**HHL**	7.1 ±0.65	0.7 ±0.1
Hemoglobin	12 ±1.3 (14 ±2 at pH 7)	0.84 ±0.05 (1.38 ±0.5 at pH 7)
Cytochrome C	49.1 ±5.3 (58.1 ±7.5 at pH 7)	1.13 ±0.09 (2.1 ±1 at pH 7)
Hemin	$1.7 \times 10^{-5} \pm 0.06 \times 10^{-5}$	$2.5 \times 10^{-5} \pm 0.2 \times 10^{-5}$

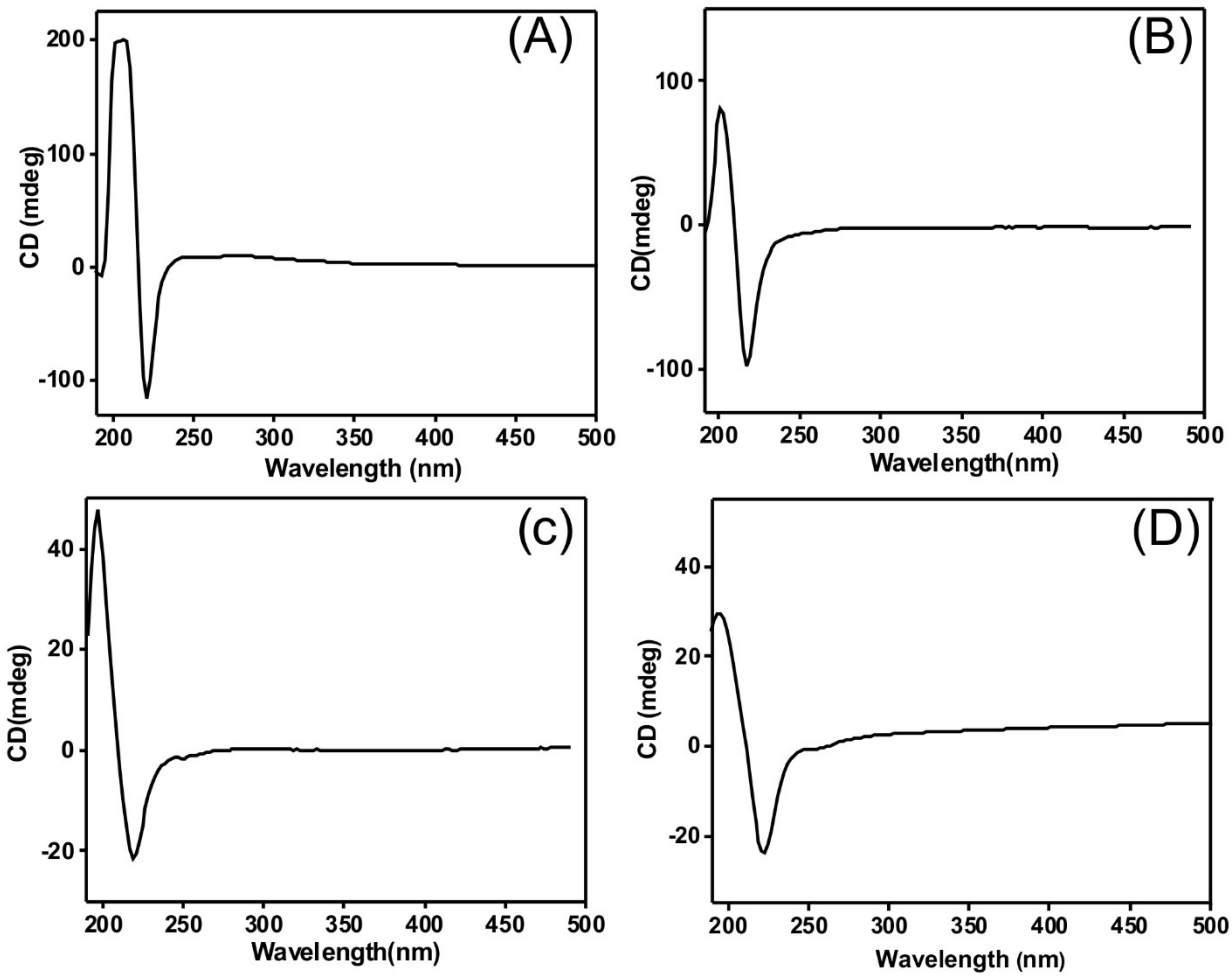

Figure S1. CD spectra of the amyloid nanostructure. (A),(B),(C) (D) represent the CD spectra of **HL**, **KL**, **HE**, **HHL** respectively.

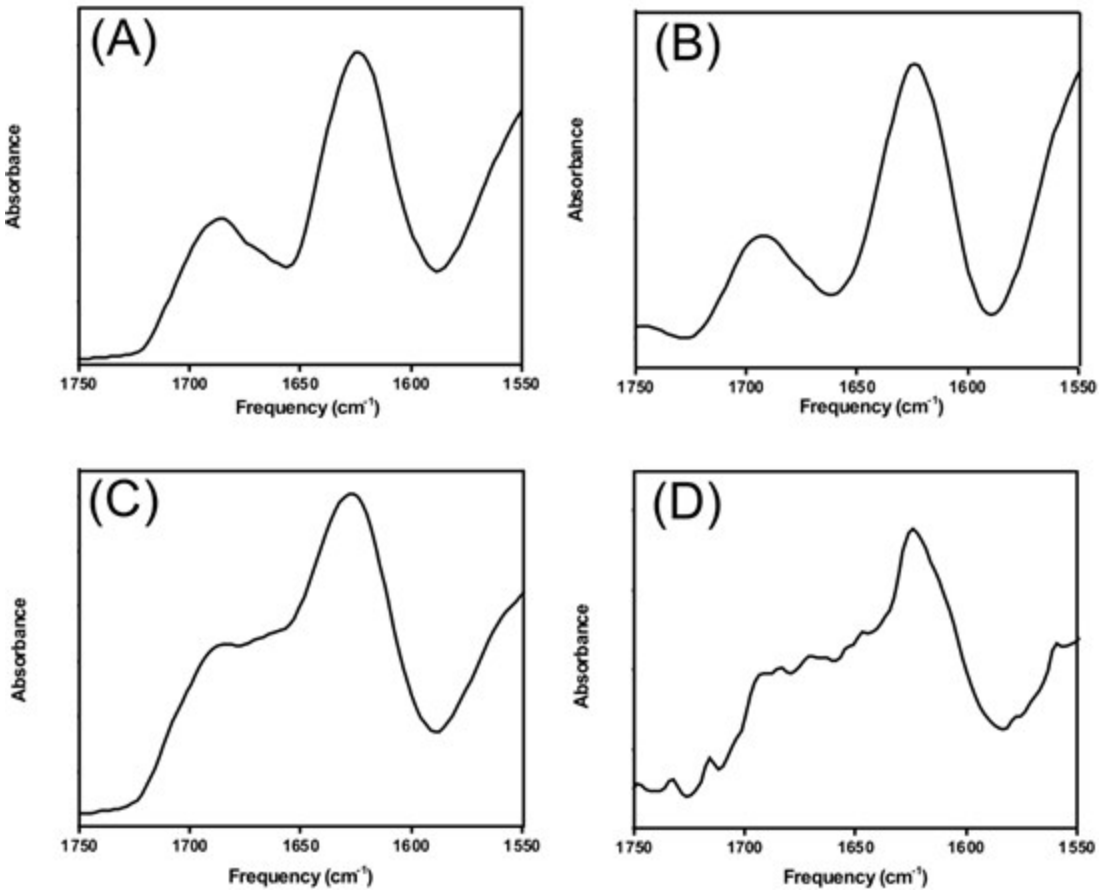

Figure S2. FTIR spectra of the amyloid nanostructure. (A),(B),(C) (D) represents the FTIR spectra of **HL**, **KL**, **HE**, **HHL** respectively.

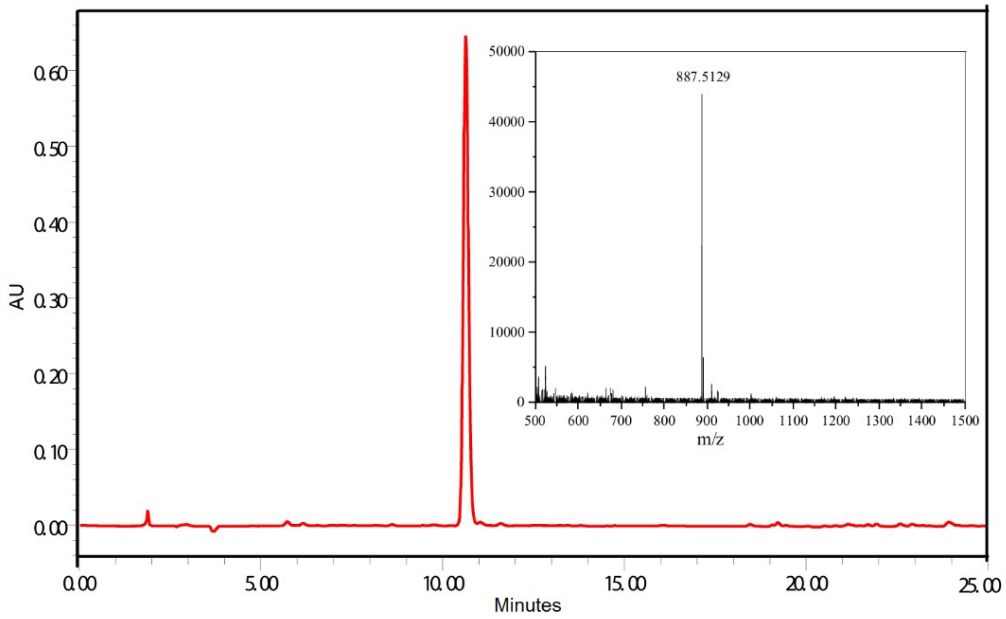

Figure S3. HPLC chromatogram of purified peptide **HL** (C_{18} Column, linear gradient from 30 to 70 % in MeCN in 20 min). Inset shows corresponding mass spectra of the purified peptide.

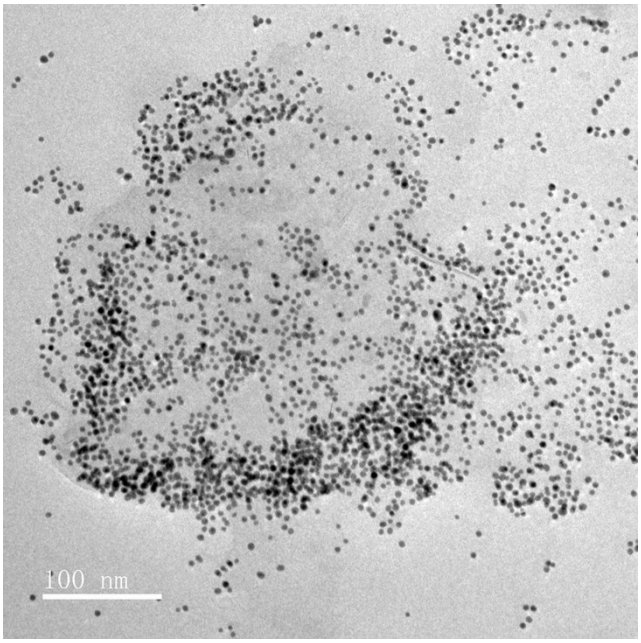

Figure S4. TEM image of negatively-charged citrate capped gold nanoparticles.

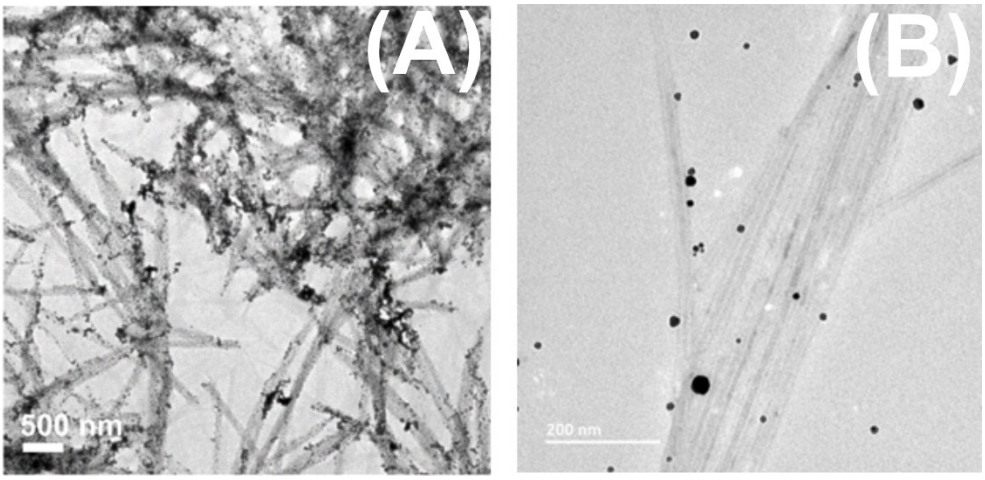

Figure S5. TEM images of A) **HL** nanotubes which were pre-incubated at pH 8 for 60 min and mixed with negatively charged gold nanoparticles (see experimental section 2.4 above). B) Positively charged gold nanoparticles incubated with **HL** nanotubes.

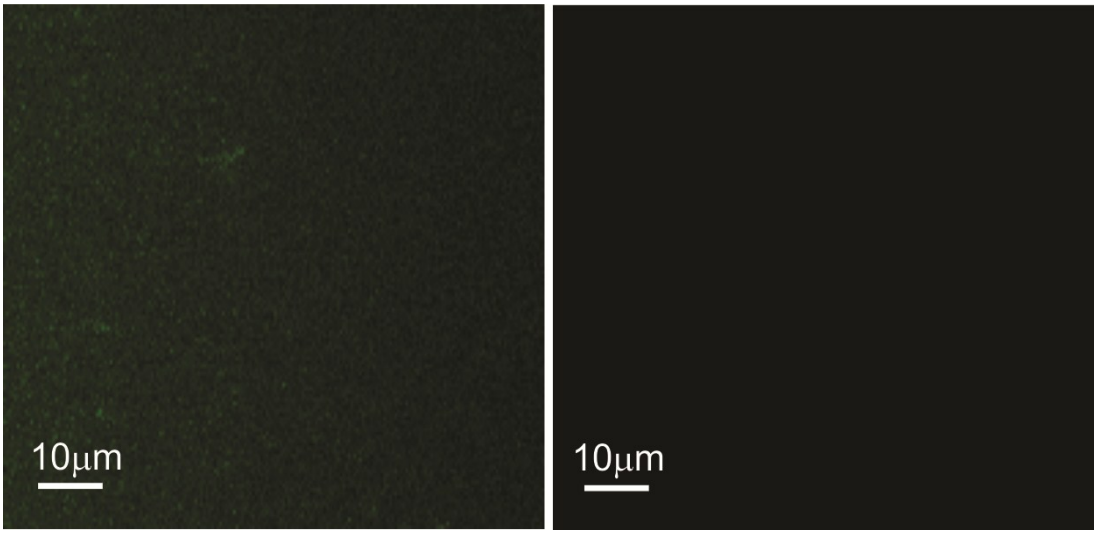

Figure S6. Confocal laser scanning microscopy images of dye without tubes (left side) and tubes without dye (right side).

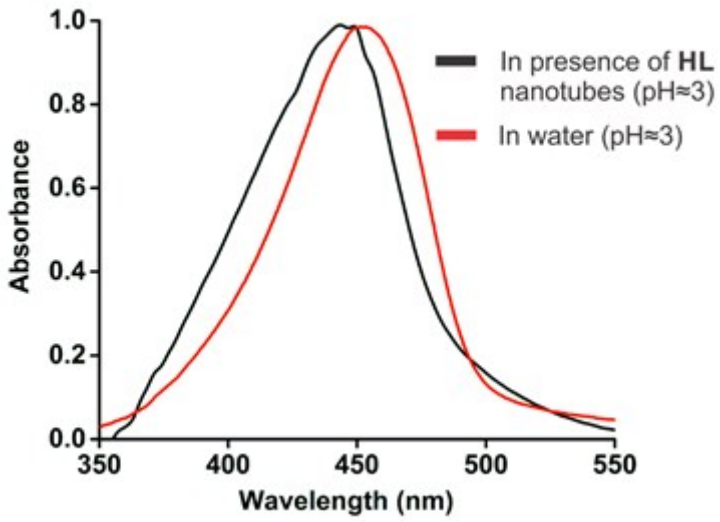

Figure S7. Normalized UV-Vis spectra of coumarin 343 in presence of **HL** nanotubes (black) and coumarin 343 in water (red) at pH ≈3.

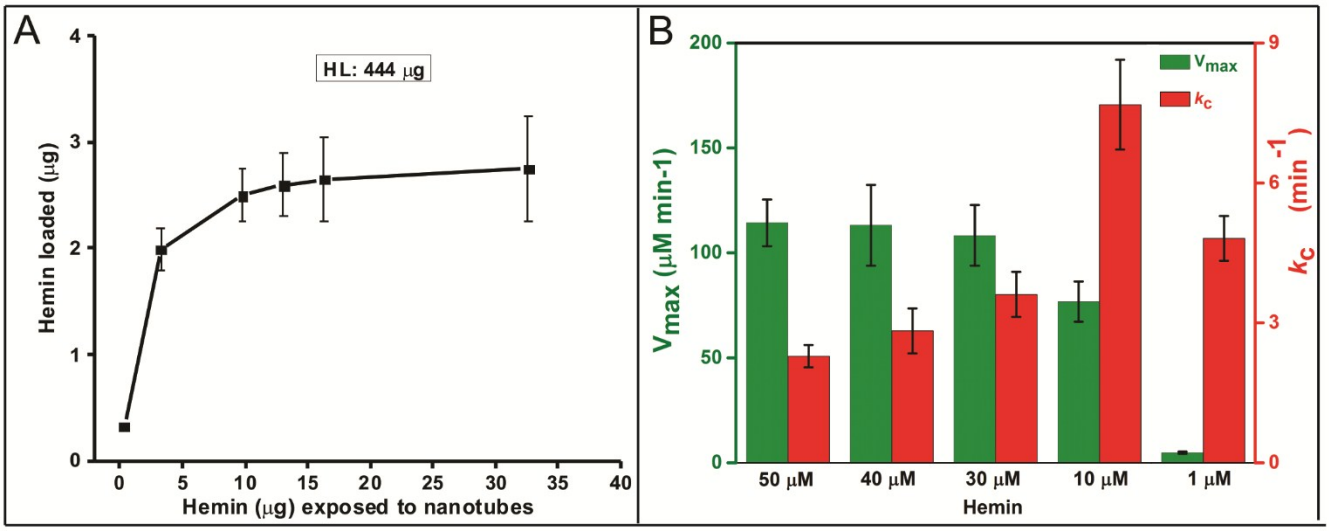

Figure S8 A) Hemin loading as a function of amount of hemin exposed to **HL** nanotubes and B) V_{max} and k_c of hemin-**HL** as a function of hemin concentration (exposed to the peptide assemblies).

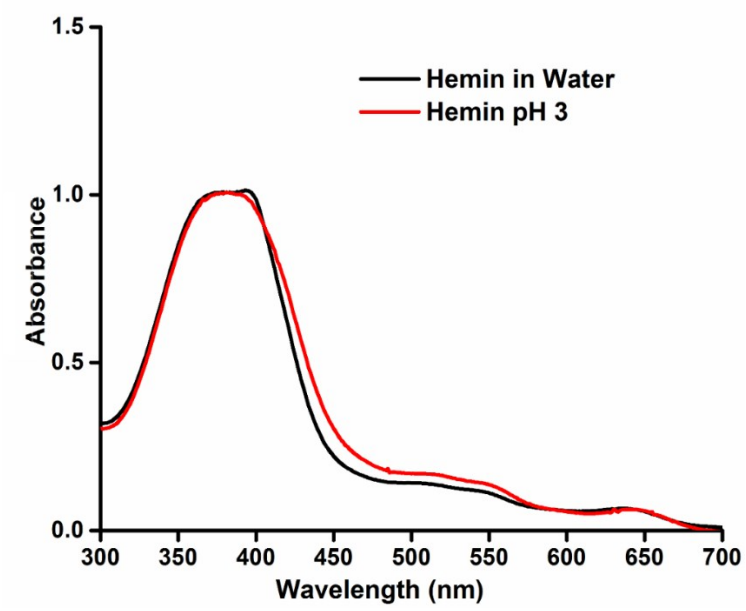

Figure S9. Normalized UV-Vis spectra of free hemin in water and free hemin in buffer (pH 3, glycine HCl).

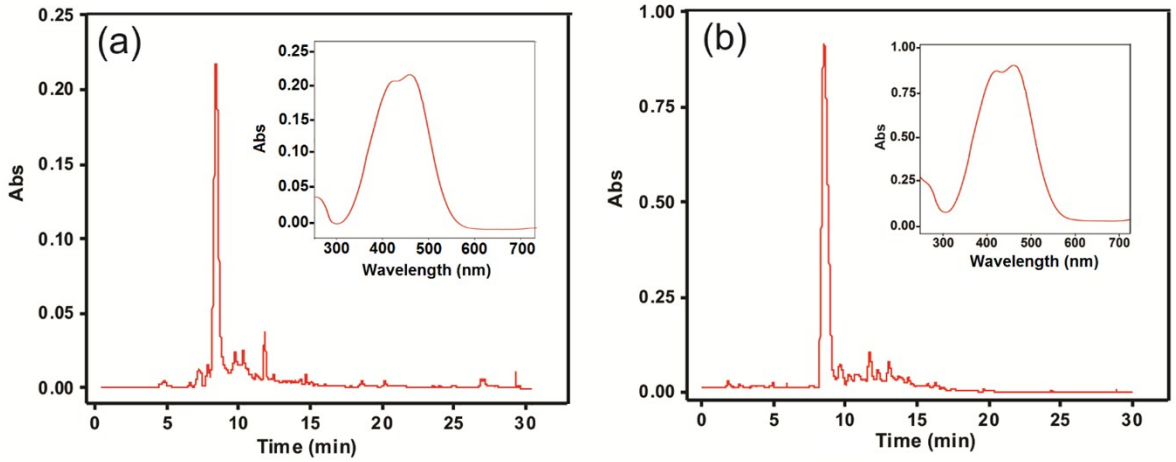

Figure S10. HPLC chromatogram (C18 Column, linear gradient from 30 to 100 % in MeCN in 20 min) and corresponding UV-Vis spectra of the major peak of methoxy phenol oxidized product by a) **HL** and b) horseradish peroxidase (**HRP**).

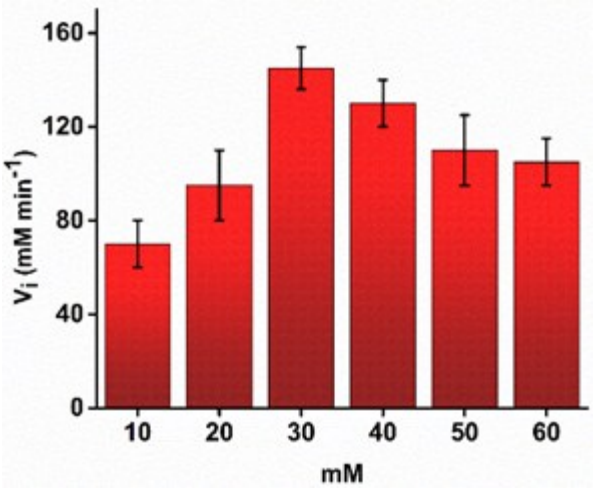

Figure S11. Initial reaction rates for the oxidation reaction of MP by **HL**. [**HL**]=1 mM, [MP]=25 mM, [H_2O_2]= 10 to 60 mM.

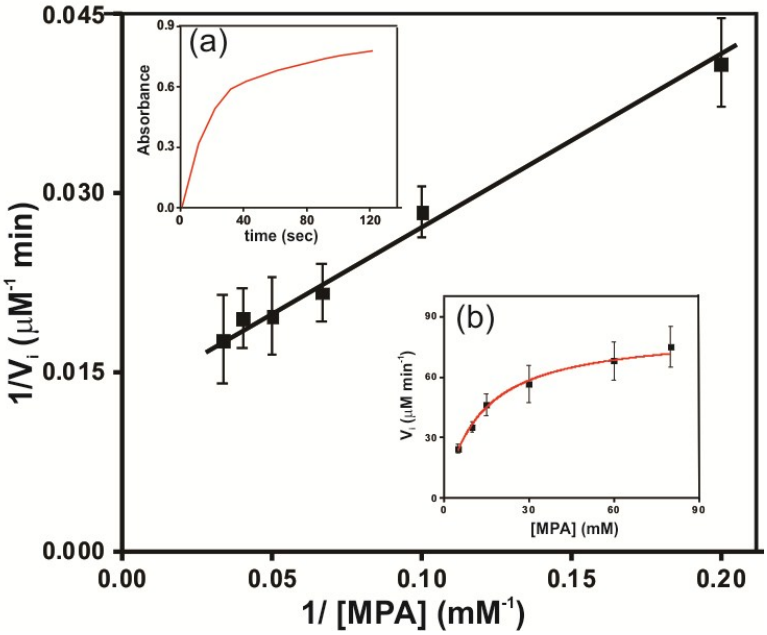

Figure S12. Representative Lineweaver-Burk plot of **HL**-hemin system. Inset shows (a) time course kinetics of cascade reaction at 25 mM MPA concentration (b) Michaeilis-Menten fitting for **HL**-hemin system.

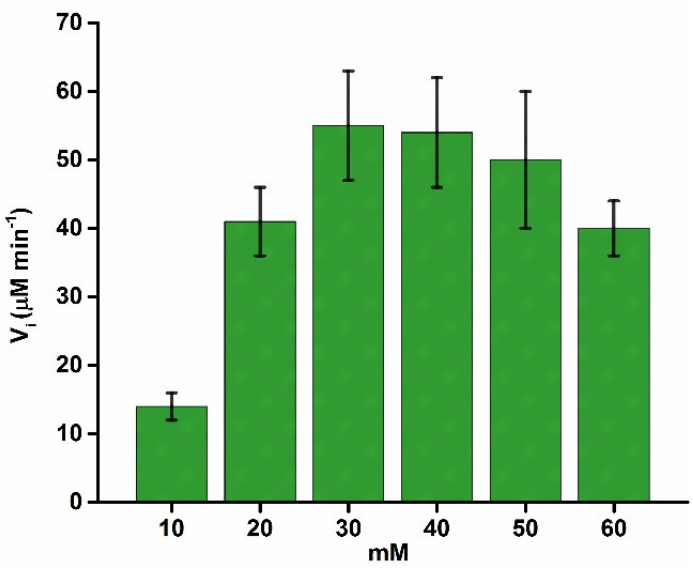

Figure S13. Initial reaction rates for the cascade reaction of MPA by **HL**. [**HL**]=1 mM, [MP]=25 mM, [H_2O_2]= 10 to 60 mM.

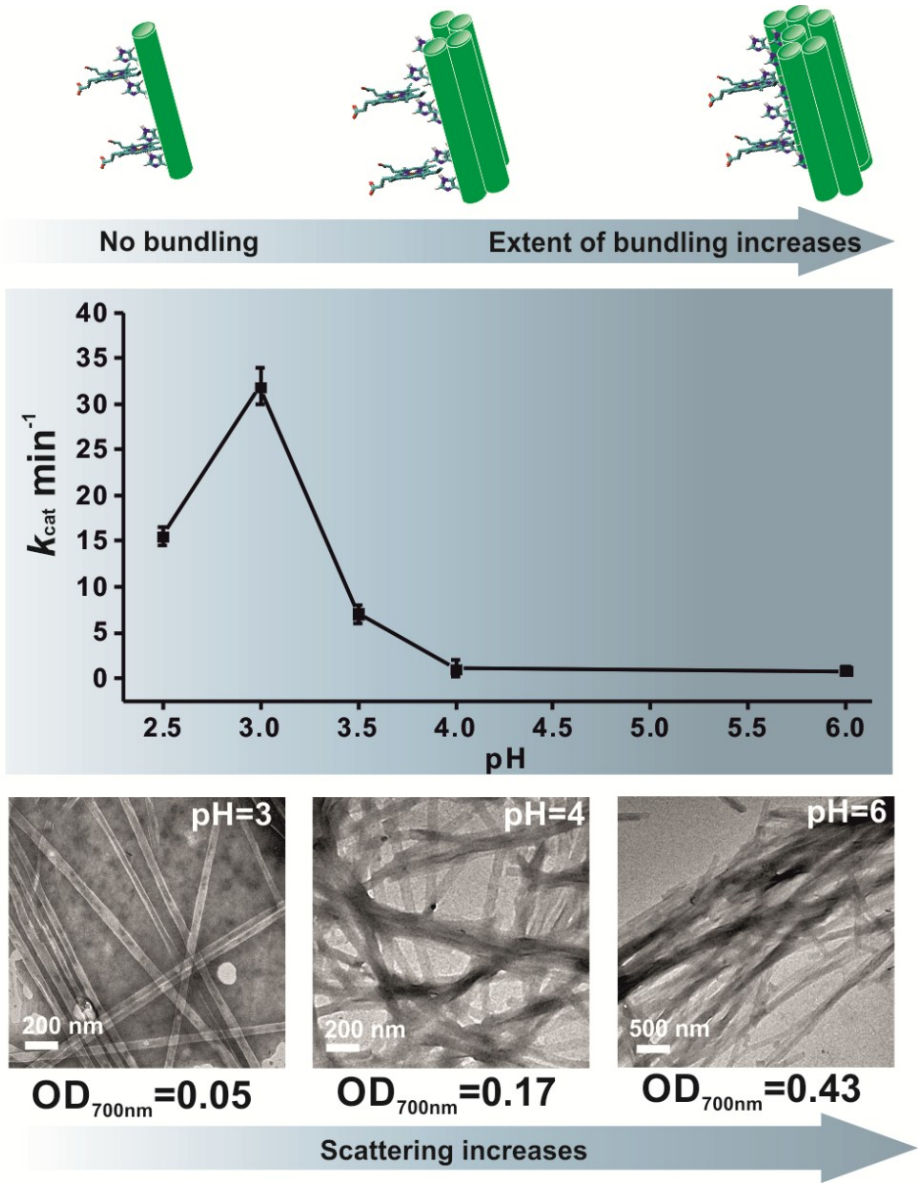

Figure S14. k_c of hemin bound **HL** nanotubes as a function of pH. TEM images showing bundling and changes of OD of **HL** nanotubes from pH 3 to 6 (left to right). OD values for scattering were noted at λ=700 nm by adding the peptides in cuvette of 10 mm path length.

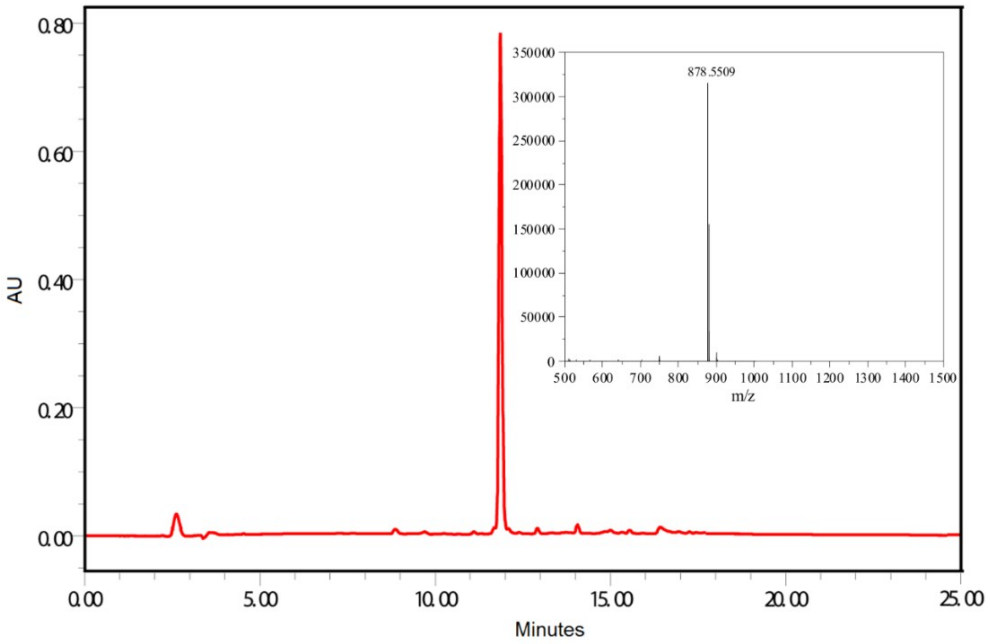

Figure S15. HPLC chromatogram of purified peptide **KL** (C_{18} Column, linear gradient from 30 to 70 % in MeCN in 20 min). Inset shows corresponding mass spectra of the purified peptide.

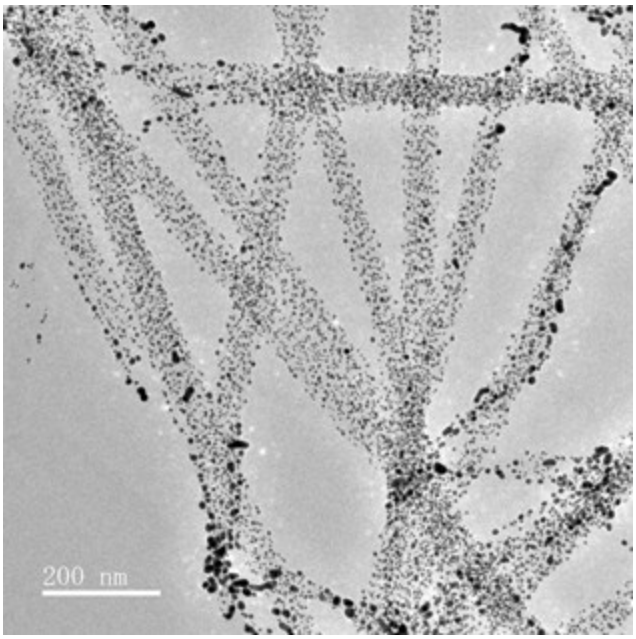

Figure S16.TEM image of negatively charged gold nanoparticles incubated with **KL**.

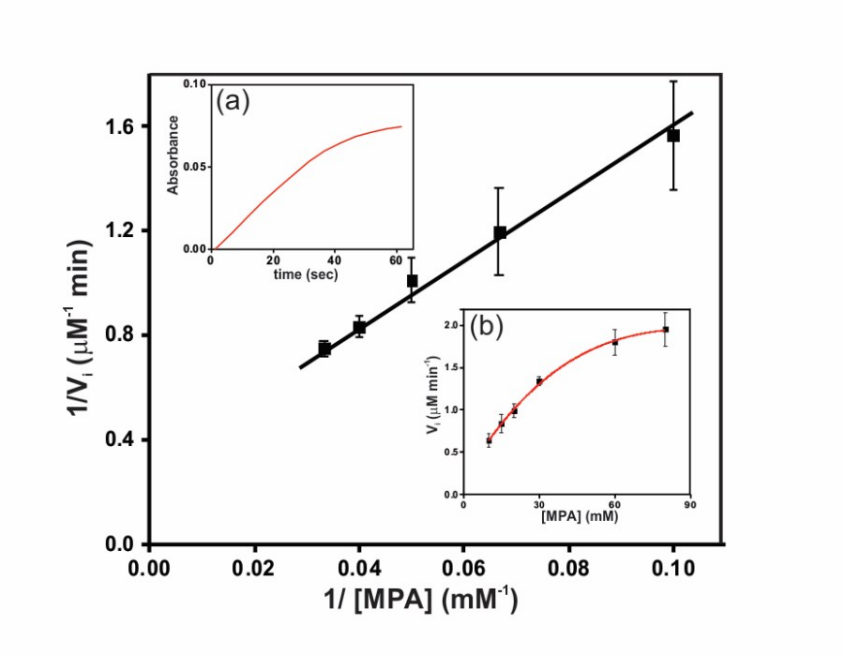

Figure S17. Representative Lineweaver-Burk plot of **KL**-hemin in presence of histidine. Inset shows (a) time course kinetics of cascade reaction at 25 mM MPA concentration (b) Michaeilis-Menten fitting for **KL**-hemin in presence of histidine.

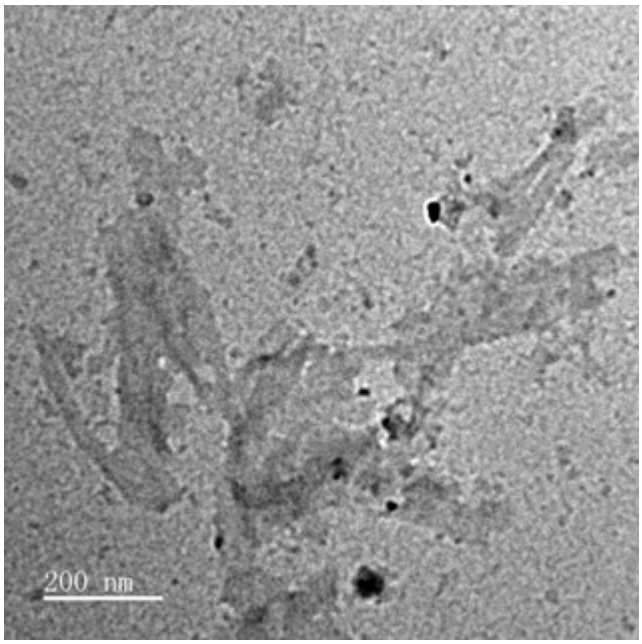

Figure S18. Representative TEM image of HFIP treated **HL**.

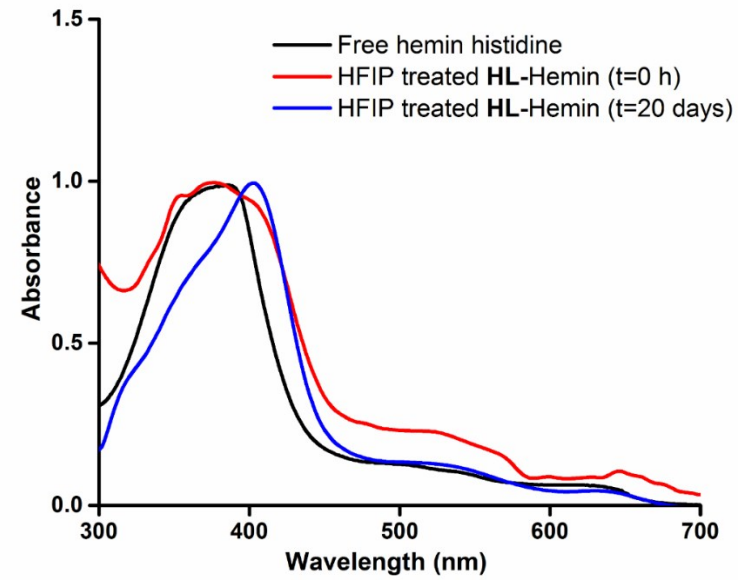

Figure S19. Normalized UV-Vis spectra of free hemin histidine at pH 3 and hemin in presence of HFIP treated **HL** at t≈ 0 h and t≈ 20 days.

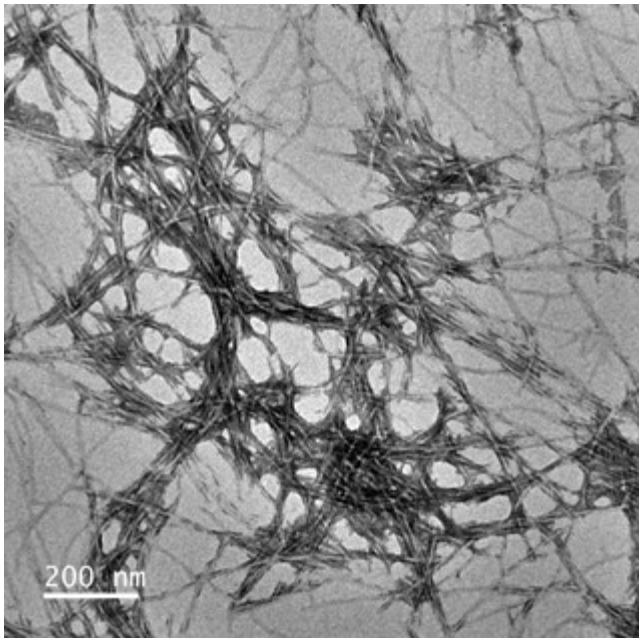

Figure S20. TEM image of **HE**.

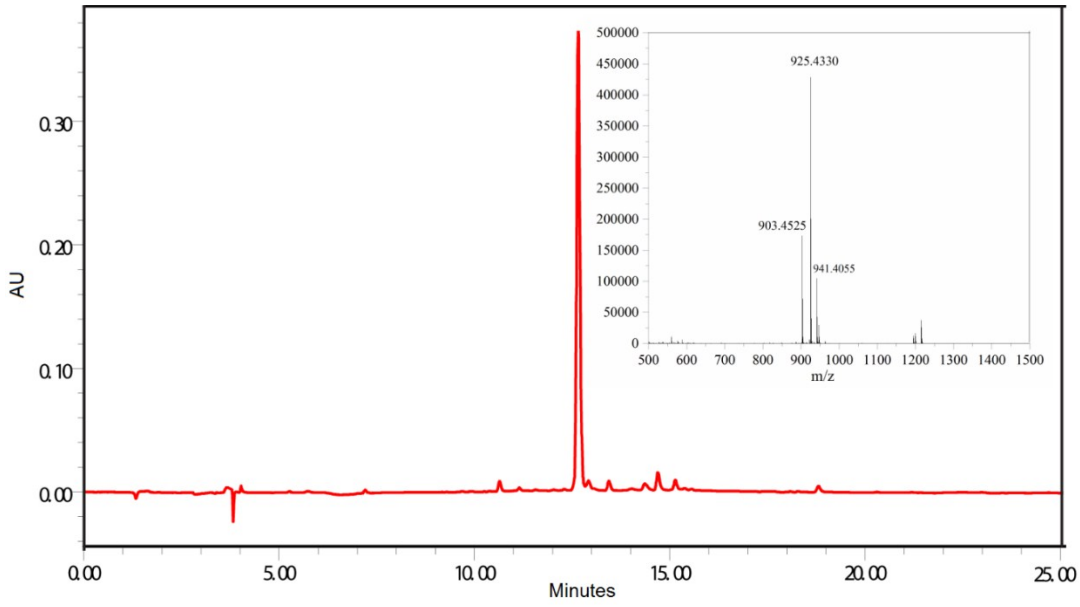

Figure S21. HPLC chromatogram of purified peptide **HE** (C_{18} Column, linear gradient from 30 to 70 % in MeCN in 20 min). Inset shows corresponding mass spectra of the purified peptide.

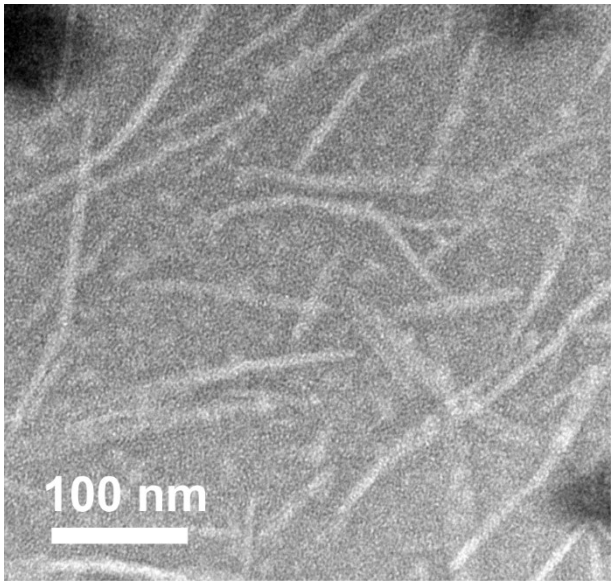

Figure S22. TEM image of **HHL.**

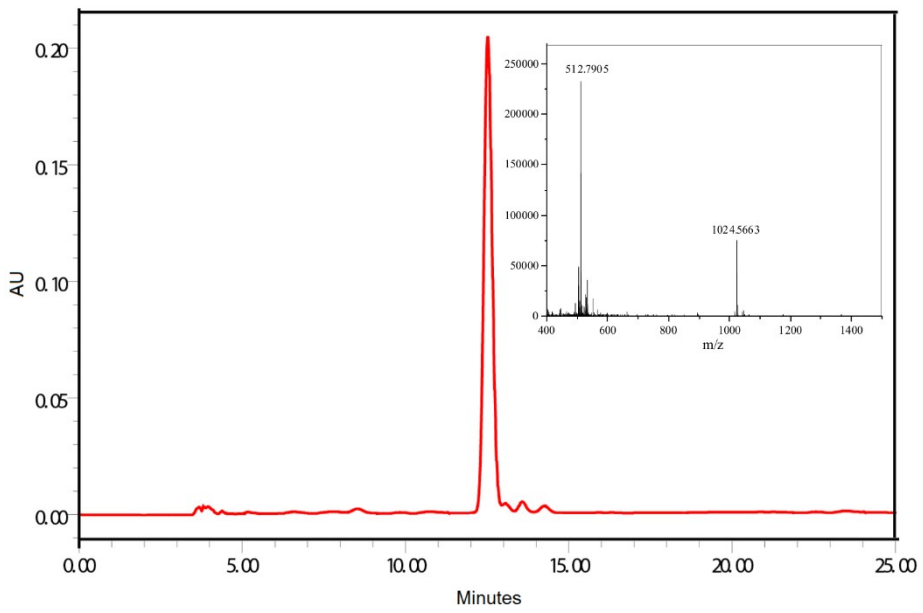

Figure S23. HPLC chromatogram of purified peptide **HHL** (C_{18} Column, linear gradient from 30 to 60 % in MeCN in 20 min). Inset shows corresponding mass spectra of the purified peptide.

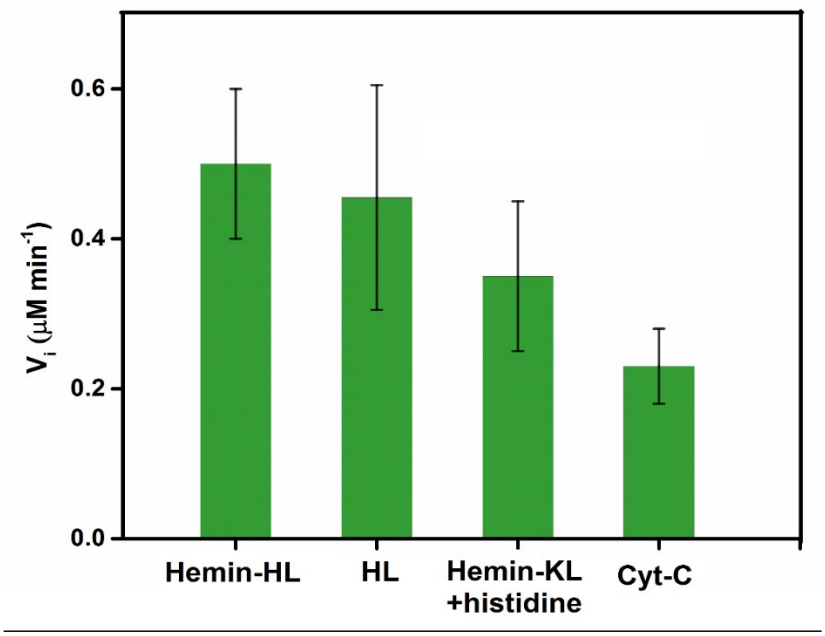

Figure S24. Initial reaction rates for the hydrolysis of MPA in different systems.

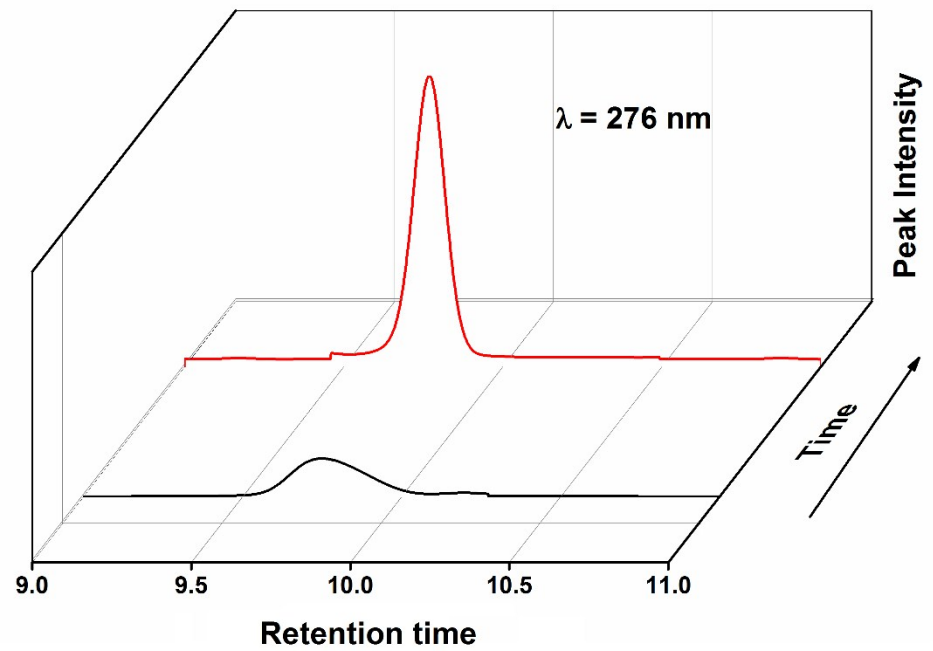

Figure S25. Time dependent HPLC chromatogram of methoxy phenol formation kinetics by peptide nanotubes.

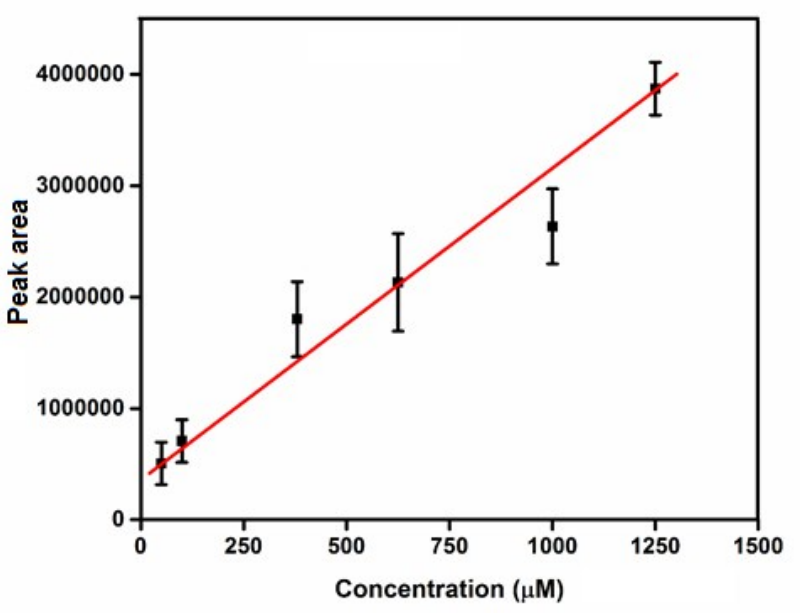

Figure S26. Standard curve for methoxy phenol (MP) from HPLC.

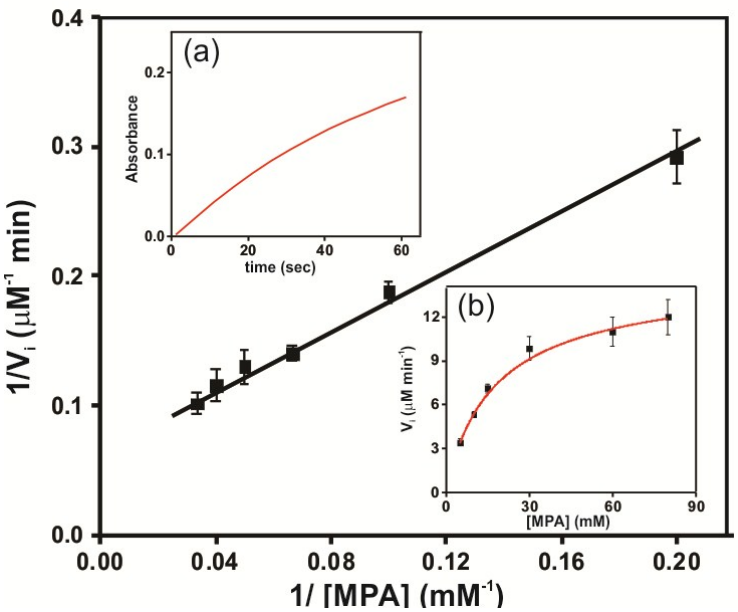

Figure S27. Representative Lineweaver-Burk plot of histidine-hemin freely diffusing system. Inset shows (a) time course kinetics of cascade reaction at 25 mM MPA concentration (b) Michaeilis-Menten fitting for histidine-hemin freely diffusing system.

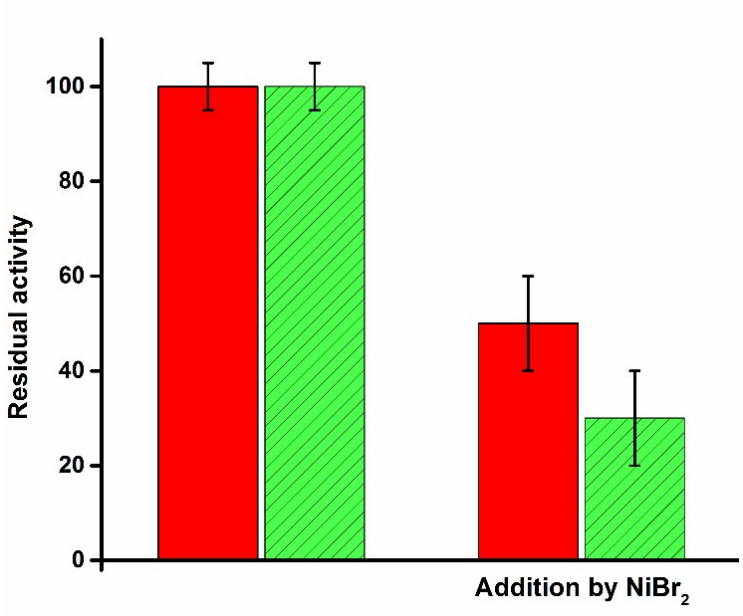

Figure S28. Residual activity of the free hemin-histidine system (green) and hemin bound **HL** (red) challenged by inhibitor $NiBr_2$ for the oxidation step.

Reference:

1) S. Li, A. N. Sidorov, A. K. Mehta, A. J. Bisignano, D. Das, W. S. Childers, E. Schuler, Z. Jiang, T. M. Orlando, K. Berland and D. G. Lynn, *Biochemistry,* 2014, **53**, 4225-4227.
2) a) N. Kapil, A. Singh, M. Singh and D. Das, *Angew. Chem., Int. Ed.,* 2016, **55***,* 7772-7776; b) N. Kapil, A. Singh and D. Das, *Angew. Chem., Int. Ed.,* 2015, **54**, 6492–6495.
3) a) G. R. Souza, C. S. Levin, A. Hajitou, R. Pasqualini, W. Arap and J. H. Miller, *Anal. Chem.,* 2006, **78**, 6232–6237; b) K.-S. Ock, U. Dembereldorj, J. Park, E.-O. Ganbold, S. Kim, H.-C. Shin and S.-W. Joo, *Spectrochim. Acta, Part A*, 2013, **102**, 419 —424.
4) a) W. C. Johnson Jr., *Annu. Rev. Biophys. Chem.,* 1988, **17**, 145; b) S. M. Kelly, T. J. Jess and N. C. Price, *Biochim. Biophys. Acta*, 2005, **1751**, 119–139.
5) A. K. Mehta, K. Lu, W. S. Childers, Y. Liang, S. N. Dublin, J. Dong, J. P. Snyder, S. V. Pingali, P. Thiyagarajan and D. G. Lynn, *J. Am. Chem. Soc.*, 2008, **130**, 9829–9835.
6) a) S. Deepa and A. K. Mishra, *J. Pharm. Biomed. Anal.*, 2005, **38**, 556–563; b) S. Chandrasekaran, Y. Sameena, I. V. M. V. Enoch, *J Incl. Phenom. Macro*., 2015, **81**, 225–236; c) G. Jones and M. A. Rahman, *J. Phys. Chem.,* 1994, **98**, 13028.
7) a) X. Wang, C. Wang, M. Pan, J. Wei, F. Jiang, R. Lu, X. Liu, Y. Huang and F. Huang, ACS Appl. Mater. Interfaces, 2017, 9, 25387–25396; b) Q. Liu, H. Wang, X. Shi, Z. Wang and B. Ding, ACS Nano, 2017, 11, 7251–7258.
8) a) Q. Wang, Z. Yang, X. Zhang, X. Xiao, C. K. Chang and B. Xu, *Angew. Chem., Int. Ed*., 2007, **46***,* 4285-4289; b) A. Liese, K. Seelbach and C. Wandrey, *Industrial Biotransformations: A Collection of Processes,* Wiley-VCH Darmstadt, 2000; c) A. C. Maehly and B. Chance, *Methods Biochem Anal.,* 1954, **1**, 357-424.
9) K. J. Laidler, *Chemical Kinetics*, Pearson Education, New Delhi, 1987.
10) A. J. Cornish-Bowden, *Principles of Enzyme Kinetics,* Butterworths, London, 1976.

11) K. J. Laidler and P. S. Bunting, *The Chemical Kinetics of Enzyme Action*, *2nd ed.*, Clarendon, Oxford, 1973.
12) W. P. Jencks, *Catalysis in Chemistry and Enzymology*, McGraw-Hill, New York, 1969.
13) N. Jura, N. F. Endres, K. Engel, S. Deindl, R. Das, M. H. Lamers, D. E. Wemmer, X. Zhang and J. Kuriyan, *Cell,* 2009, **137**, 1293– 1307.
14) X. Zhang, J. Gureasko, K. Shen, P. A. Cole and J. Kuriyan, *Cell,* 2006, **125**, 1137-1149.